



ORIGINAL RESEARCH ARTICLE

Effect of Induction Quenching and Tempering Temperature on the Mechanical Properties and Microstructure Evolution of 45 Steel for Linear Guide

Ying Sun, Lianfang He, Yuyang Gao, Shuo Fang, Zhichao Li, and Huiping Li

Submitted: 1 August 2023 / Revised: 17 September 2023 / Accepted: 29 September 2023

In this paper, the influence of induction quenching and tempering temperatures on the evolution of mechanical properties and microstructure of 45 steel for linear guides were investigated based on the tensile, impact, hardness tests and fracture morphology. The results indicate that the hardness of untempered and 200 °C tempered samples are higher and the difference is not significant, while the hardness of 300 and 400 °C tempered samples decrease as tempering temperature increases. Lower tensile strengths are observed in untempered and 200 °C tempered samples, which increase significantly after being tempered at 300 °C and then decrease slightly after being tempered at 400 °C. As the tempering temperature remains constant, the impact toughness value steadily declines as the quenching temperature rises, whereas when the quenching temperature remains constant, the impact toughness increases as the tempering temperature rises. The optimum induction quenching temperature was finally determined to be 850-900 °C, and the optimum tempering temperature was 300 °C. The findings of this study can be used to develop technical guidelines for the design of induction hardening and tempering process parameters for linear guides.

Keywords induction hardening, mechanical properties, microstructure evolution, tempering temperature

1. Introduction

Rolling linear guides have gradually replaced traditional sliding linear guides due to their low coefficient of friction, high positioning precision, and preferable accuracy retention (Ref 1, 2). The stiffness, friction, and motion accuracy of rolling linear guides will directly affect the load-carrying performance and motion accuracy of high-end CNC machine tools and precision instruments. Improving the performance and reliability of linear guides has become an urgent task in the advancement of CNC technology and machine tools (Ref 3-5). The contact surfaces between the linear guides and steel balls are subjected to tremendous pressure during operation, resulting in the wear of linear guides. Therefore, great hardness and wear resistance are required for the contact surfaces (Ref 6, 7). The required performance can be achieved through reasonable material selection and appropriate surface heat treatment procedures, which improve the service life of parts (Ref 8, 9). Considering the working conditions, performance requirements, cost and feasibility of heat treatment process, 45 steel is selected as the raw material of linear guides, and the comprehensive mechan-

ical properties of the parts such as hardness, strength and wear resistance can be improved by induction hardening.

Induction hardening is characterized by high heating efficiency, high productivity, and low environmental pollution (Ref 10). The parts after induction hardening display outstanding overall mechanical properties, exhibiting excellent plasticity and toughness inside and strong wear resistance and fatigue strength on the surface (Ref 11). Numerous studies have been conducted on the induction hardening of 45 steel. Liu et al. (Ref 12) comparatively studied the structure of the hardened layers in 45 steel, as well as the corrosion resistance and electrical conductivity under the two quenching methods of induction hardening and laser phase transformation hardening. In order to compare the effects of the two tempering techniques on mechanical characteristics and microstructure, Feng et al. (Ref 13) performed microstructure observation and hardness tests on the 45 steel seamless steel pipes tempered by conventional heating and induction heating. Li et al. (Ref 14) used the cooling rate as a variable to investigate the evolution law of microstructure and mechanical properties of 45 steel after induction hardening. Kurek et al. (Ref 15) calculated the change of temperature field and electromagnetic field of 45 steel during induction hardening by numerical simulation.

Due to the inhomogeneous temperature distribution and phase transition between surface layer and inner area during induction heating and water spray cooling, parts after induction hardening are prone to quenching distortion and residual stress (Ref 16-18). In order to reduce the impact of quenching residual stress, parts need to be tempered at low or medium temperatures to transform the martensite in the surface hardened layer into tempered martensite with better comprehensive properties, thereby improving toughness. The temperature used for induction quenching and tempering has a significant effect on the evolution of microstructure and

Ying Sun, Lianfang He, Yuyang Gao, Shuo Fang, Zhichao Li, and Huiping Li, School of Materials Science and Engineering, Shandong University of Science and Technology, Qingdao 266590 Shandong, China. Contact e-mails: If he2007@126.com, lizhichao198918@163.com, and lihuiping99@163.com.

mechanical properties. In this paper, different heat treatment process parameters were used to conduct induction quenching and tempering experiments. The purpose of the study described here is to determine the optimal induction quenching and tempering temperatures of 45 steel for linear guides. Mechanical properties and microstructure evolution of samples under different heat treatment conditions were compared. Results of the study described here can be used to guide the design of induction hardening and tempering process parameters for linear guides, as well as a basis for the design of quenching and tempering temperatures in the numerical simulation of induction hardening.

2. Materials and Experimental Procedure

Chemical composition of 45 steel for linear guides used in the experiment is shown in Table 1. 45 steel has excellent plasticity, toughness and machining performance, making it a suitable material for various parts such as linear guides, sprockets and ball screws.

45 steel plates with a thickness of 4 mm were selected for the experiments. Two types of samples with sizes of 4 mm × 25 mm × 145 mm and 4 mm × 15 mm × 60 mm were cut by the CNC-W2 wire electric discharge machine, which were used to process tensile and impact samples after induction hardening and tempering experiments, respectively. The original state of 45 steel used in the experiment was hot rolled and had been normalized before the start of the experiment.

For accurate measurement for the real-time temperature of samples during induction heating process, temperature measuring holes with the diameter of Ø1 mm × 2 mm were drilled on the side of samples with a bench drill to fix the K-type thermocouples. The experiment is divided into two stages, which are induction hardening and low or medium temperature tempering, and the process route of heat treatment is shown in Fig. 1. The specific heat treatment process parameters are listed in Table 2. The quenching temperatures selected in the experiment were 800, 850, 900, 950, 1000, 1050, 1100 °C, and the tempering temperatures were 200, 300, and 400 °C, respectively. In addition, a group of samples without being tempered were set for comparison.

The experimental equipment for induction hardening consists of the induction heating device (IGBT intelligent induction power supply, water circulating system and electrical control cabinet) and the data acquisition system (PicoLog data acquisition software, K-type armored thermocouple, and TC-08 temperature acquisition module), as shown in Fig. 2. The samples were heated to the quenching temperatures at a rate of 30 °C/s by IGBT intelligent induction power supply and subsequently quenched in water. The voltage is 580 V, the current is 66 A, and the frequency is 8000 Hz.

The sample was wrapped with aluminum silicate ceramic fiber cotton to reduce heat loss and then placed in the induction coil. K-type armored thermocouple was inserted into the temperature measuring hole to detect the real-time temperature, as shown in Fig. 3. The temperature curve of the sample quenched at 850 °C obtained by K-type thermocouple and TC-08 temperature acquisition module is shown in Fig. 4. In order to ensure a more even overall heat transfer, two pauses were set up during induction heating process, with each pause lasting 7-8 s.

The samples that need to be tempered were heated to 200, 300 and 400 °C and held for 5 minutes in SX2-4-10 box-type resistance furnace, and then cooled to room temperature in air. Samples with dimensions of 4 mm × 25 mm × 145 mm and 4 mm × 15 mm × 60 mm were processed into tensile and impact samples, respectively. Drawings of tensile and impact samples are shown in Fig. 5 and 6, respectively.

During the design and processing of samples, the rectangular plate should be cut out first, and the final outline of tensile and impact samples should be cut after the induction quenching and tempering experiments. On the one hand, the impact of edge effects caused by induced currents on the temperature distribution of samples can be reduced. On the other hand, the temperature measuring holes can be cut off, thus avoiding stress concentration which could affect the tensile and impact properties of samples.

In order to obtain the optimum induction quenching and tempering temperatures of 45 steel for linear guides, different heat treatment process parameters were used for induction quenching and tempering experiments, and the hardness test was carried out by 200HR-150 Rockwell hardness tester. The samples after being quenched and tempered were processed into tensile and impact samples, tensile and impact tests were performed using WDW 200E microcomputer-controlled electronic universal testing equipment and the JB-300B impact testing machine, respectively. Following the completion of tensile and impact tests, the fracture positions of samples were cut out and the fracture morphology was examined using the JXA-8230 electron probe.

3. Results and Discussion

3.1 Hardness Test

After induction quenching and tempering experiments, the hardness test was carried out, five points were taken on each sample and the average was calculated as the final hardness value. The hardness values for samples subjected to different heat treatment conditions are depicted in Fig. 7.

As shown in Fig. 7, when the quenching temperature remains constant, the hardness values of untempered and 200 °C tempered samples are higher and the difference is not significant, while the hardness values of 300 and 400 °C

Table 1 Chemical composition of 45 steel, wt.%

Mn	C	Si	Ni	Cr	Cu	Fe
0.50-0.80	0.42-0.50	0.17-0.37	≤ 0.30	≤ 0.25	≤ 0.25	Bal.

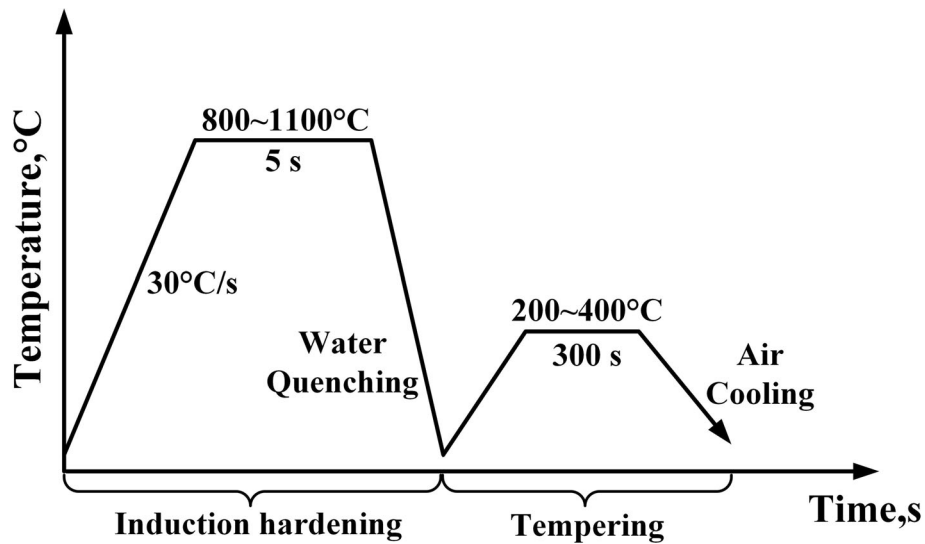


Fig. 1 Heat treatment process route

Table 2 Heat treatment process parameters

Serial number	Quenching temperature, °C	Tempering temperature, °C
1	800	...
2	800	200
3	800	300
4	800	400
5	850	...
6	850	200
7	850	300
8	850	400
9	900	...
10	900	200
11	900	300
12	900	400
13	950	...
14	950	200
15	950	300
16	950	400
17	1000	...
18	1000	200
19	1000	300
20	1000	400
21	1050	...
22	1100	...

tempered samples decrease with increasing tempering temperature. Tempering is the process of martensite decomposition (Ref 19, 20), which refers to the precipitation of supersaturated solid solution carbon from α -Fe. The higher the tempering temperature is, the more completely the martensite is decomposed, the less carbon is dissolved in α -Fe, and the weaker the solid solution strengthening effect of carbon, so the hardness will decrease with increasing tempering temperature. In addition, due to the short tempering time set in the experiment, the hardness values of 200 °C tempered samples are not significantly different from those of untempered samples.

When the tempering temperatures are the same, the hardness of the samples after being quenched at 800 °C is greater than other quenching temperatures, especially when tempering temperatures are 300 and 400 °C. Excessively high quenching temperatures cause over-burning and coarsening of the grains, making the steels more prone to fracture. The brittleness of the material increases, its toughness drops, and therefore the hardness decreases. According to the technical requirements of linear guides, the hardness value after heat treatment ranges from 56 to 60 HRC. Therefore, according to Fig. 7, the hardness values of 400 °C tempered samples are lower than 54

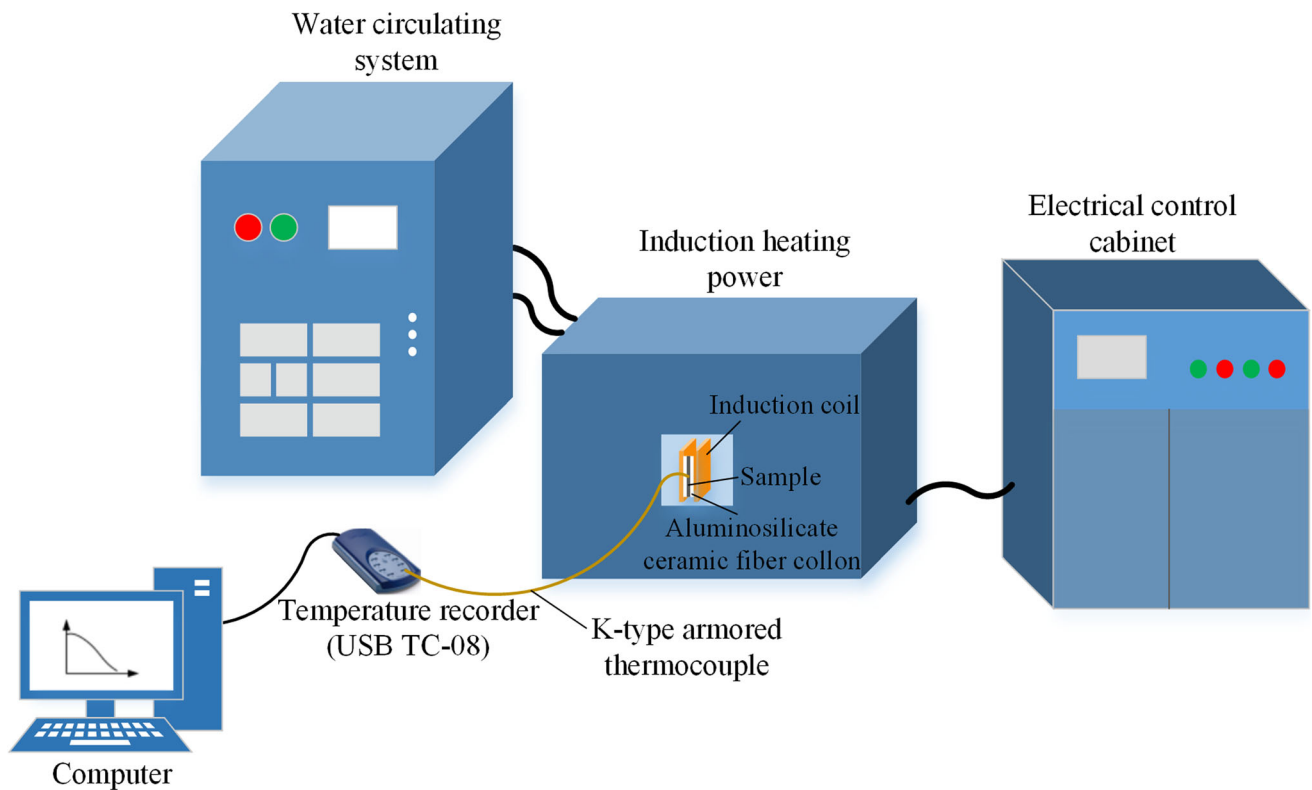


Fig. 2 Schematic of induction hardening experimental equipment

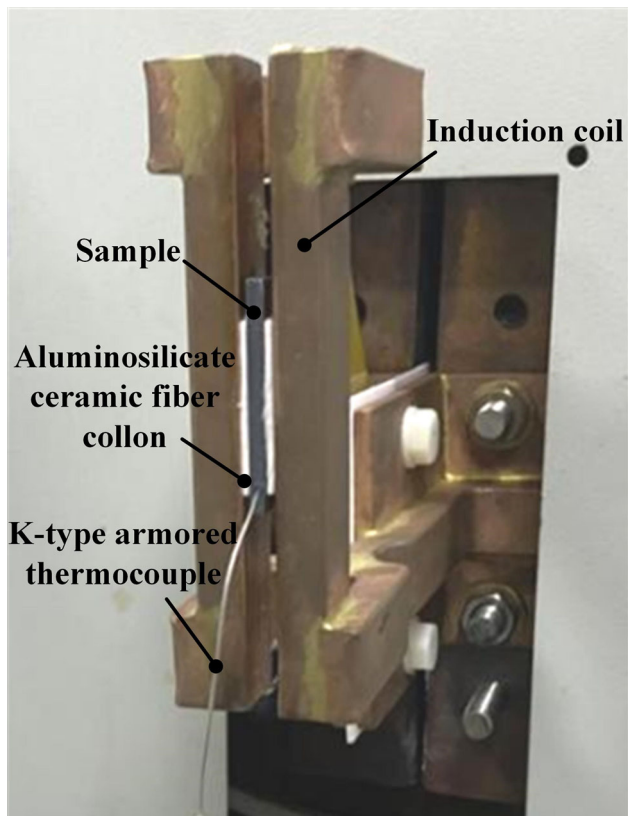


Fig. 3 Installation diagram of the samples

HRC, which cannot meet the technical requirements of linear guides.

3.2 Tensile Mechanical Properties and Fracture Mode Analysis

3.2.1 Tensile Strength. Tensile samples were processed after induction quenching and tempering experiments, and the uniaxial tensile test was conducted to obtain the evolution law of the tensile strength under different tempering and quenching temperatures, as shown in Fig. 8.

Tensile strength values of samples under different heat treatment conditions are depicted in Fig. 8. Tensile strength values of untempered and 200 °C tempered samples are lower and the difference is not significant. This is because the tempering temperature of 200 °C is relatively low and the holding time of 5 minutes is short, which is not conducive to the dissolution of carbon in martensite, resulting in no significant change in tensile strength. Tensile strength values of 300 °C tempered samples increase significantly, which is approximately 2 to 3 times those of the untempered samples. It is because the supersaturated carbon dissolved in the martensite will precipitate ϵ -carbides at the tempering temperature of 300 °C, which play a role in secondary hardening (Ref 21), so the tensile strength increases significantly. When tempered at 400 °C, the degree of carbon precipitation in martensite continued to increase, and the tensile strength decreased slightly compared with those tempered at 300 °C.

When the quenching temperature is 1000 °C, tensile strength gradually increases with increasing tempering temperature, which differs from the changing trend at the quenching

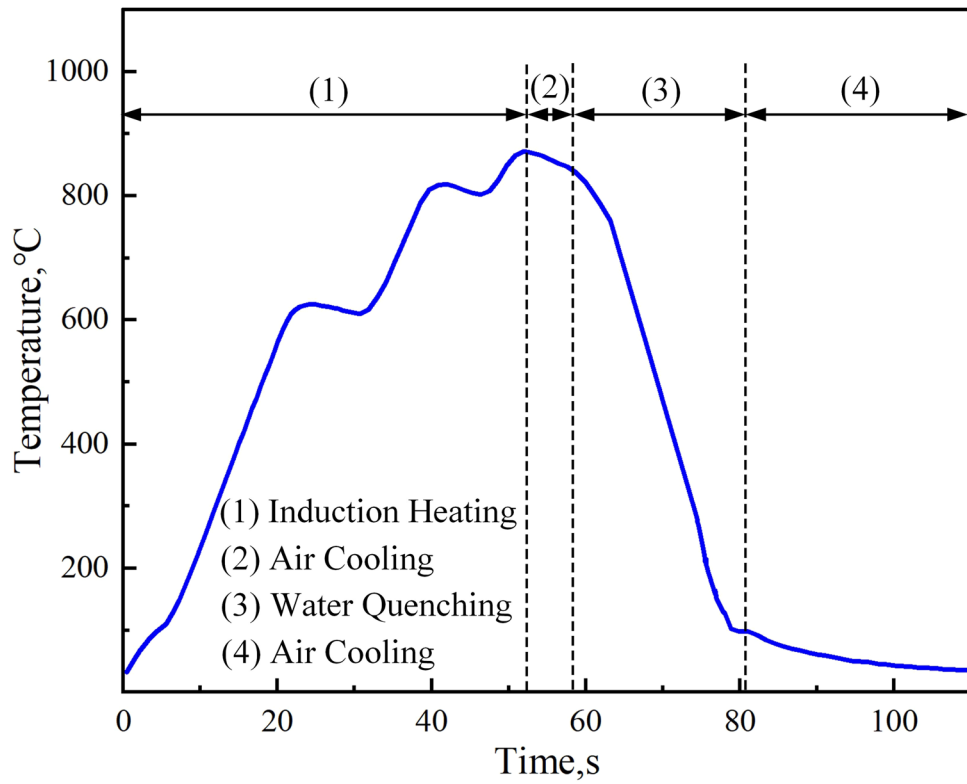


Fig. 4 Temperature curve of induction hardening process

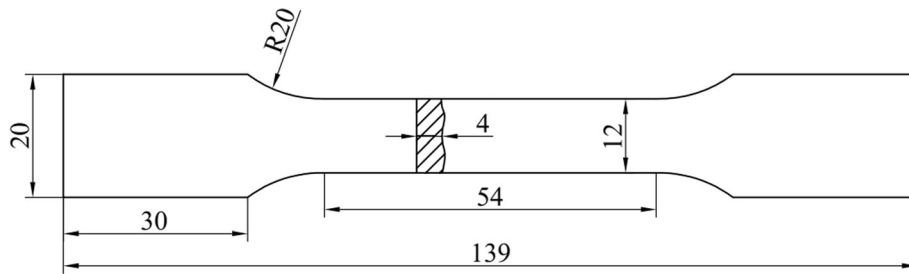


Fig. 5 Drawing of tensile samples (mm)

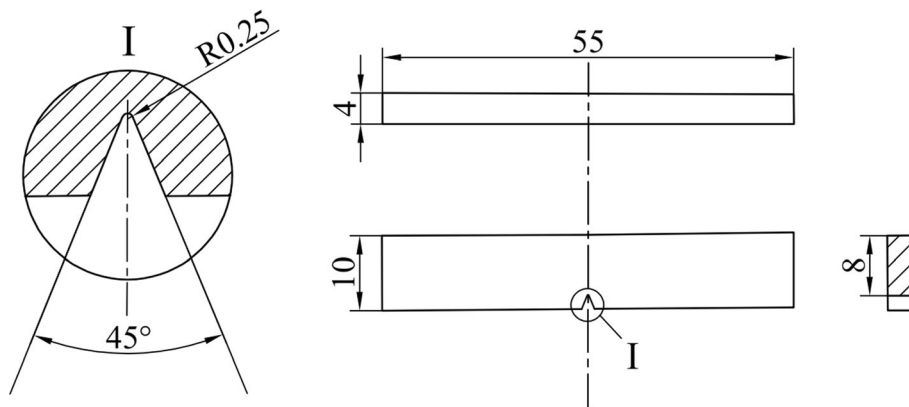


Fig. 6 Drawing of impact samples (mm)

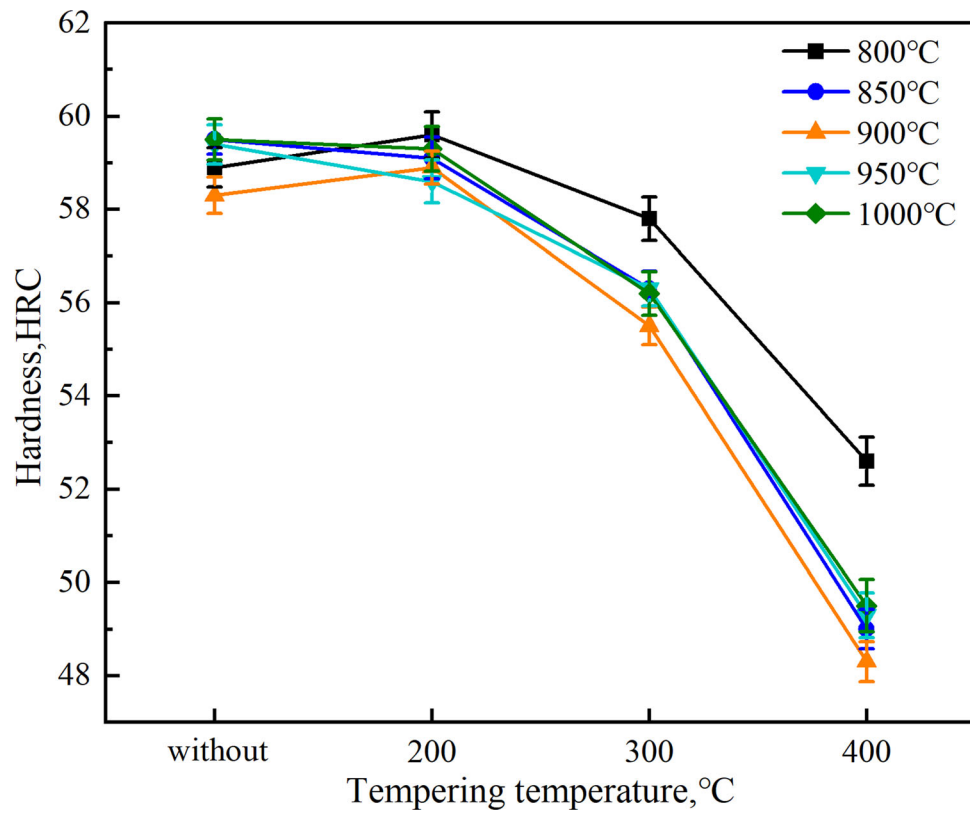


Fig. 7 Hardness of samples under different heat treatment conditions

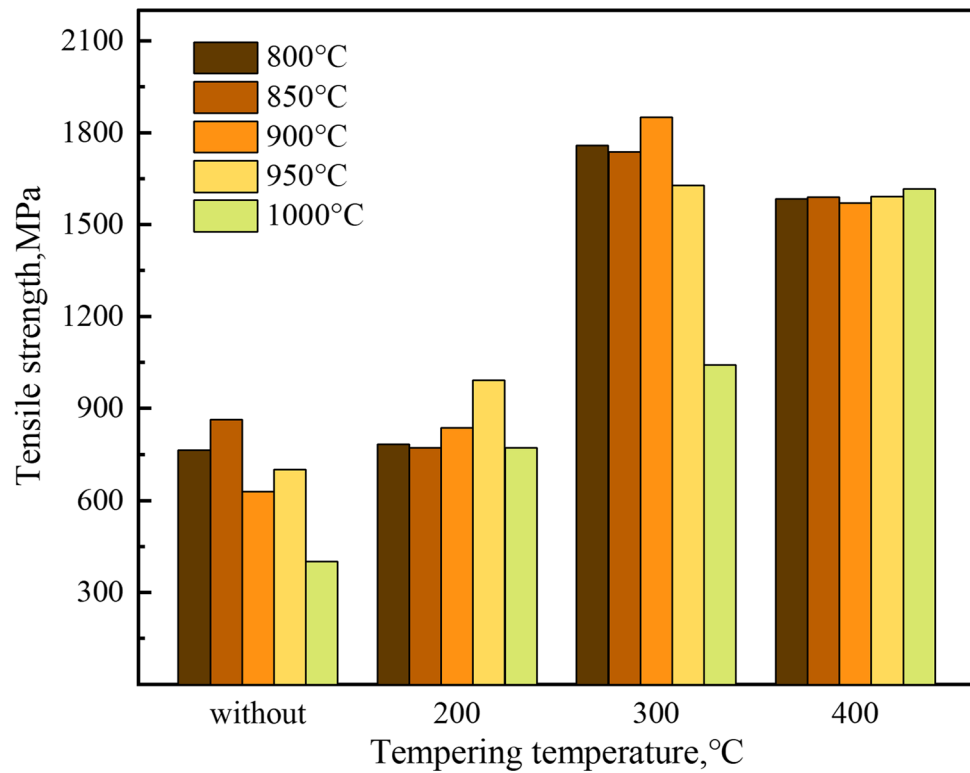


Fig. 8 Tensile strength under different heat treatment conditions

temperature of 800-950 °C. The increase in quenching temperature enhances the incorporation of carbon and additional alloying elements into austenite, as well as its homogeneity, which benefits the improvement of tensile strength. Meanwhile, the increase in quenching temperature will cause the size of austenite grains to increase (Ref 22), and the coarse austenite grains can lead to a decrease in strength (Ref 23). The growth of austenite grains plays a leading role during high-temperature quenching, so the tensile strength of samples quenched at 1000 °C shows a different changing trend from that of other samples.

3.2.2 Tensile Fracture Morphology. The morphologies of tensile fracture in untempered and 300 °C tempered samples are presented in Fig. 9. It can be seen from Fig. 9 that the untempered samples exhibit brittle fracture mode. When the quenching temperature is lower, the tensile fracture does not show obvious intergranular fracture characteristics. As the temperature for quenching increases, the size of grains gradually grows (Ref 24).

As shown in Fig. 9(i) and 10, when the quenching temperature is equal to or higher than 1000 °C, the grain size increases, obvious smooth cleavage planes can be seen from the fracture, and the cracks propagate along the grain boundaries, showing typical intergranular fracture characteristics (Ref 25, 26). For the 300 °C tempered samples, micropore-accumulated dimples begin to appear in the tensile fracture, accompanied by partial quasi-cleavage fracture features (Ref 27). The toughness of the material is improved, and the risk for intergranular cracking is reduced.

3.3 Impact Performance and Fracture Mode Analysis

3.3.1 Impact Toughness. Impact samples were processed after induction tempering and quenching experiments, and the impact test was conducted to obtain the evolution law of the impact toughness under different tempering and quenching temperatures, as shown in Fig. 11.

Impact toughness reflects the toughness of the material, the higher the impact toughness value, the better the toughness of the material. As shown in Fig. 11, impact toughness values of the samples follow clear rules. When the tempering temperature remains constant, the impact toughness value steadily declines as the quenching temperature rises, indicating that the toughness of the material decreases gradually. There will be more carbides dissolved in austenite as the quenching temperature rises, and the stability of the austenite will be enhanced. After quenching, austenite transforms into martensite. The increase in carbon concentration in martensite will lead to an increase in hardness and a decrease in toughness.

In the case of constant quenching temperature, the impact toughness values of the samples increase as the tempering temperature rises, indicating that the toughness of the material is improved gradually. It is related to the precipitation of carbides in martensite (Ref 28), the higher the tempering temperature, the more active the carbon atoms are, which is conducive to the precipitation of carbides (Ref 29), resulting in the decrease in hardness and increase in toughness.

3.3.2 Impact Fracture Morphology. The morphologies of impact fracture in untempered and 300 °C tempered samples are summarized in Fig. 12. According to Fig. 12, fracture mode

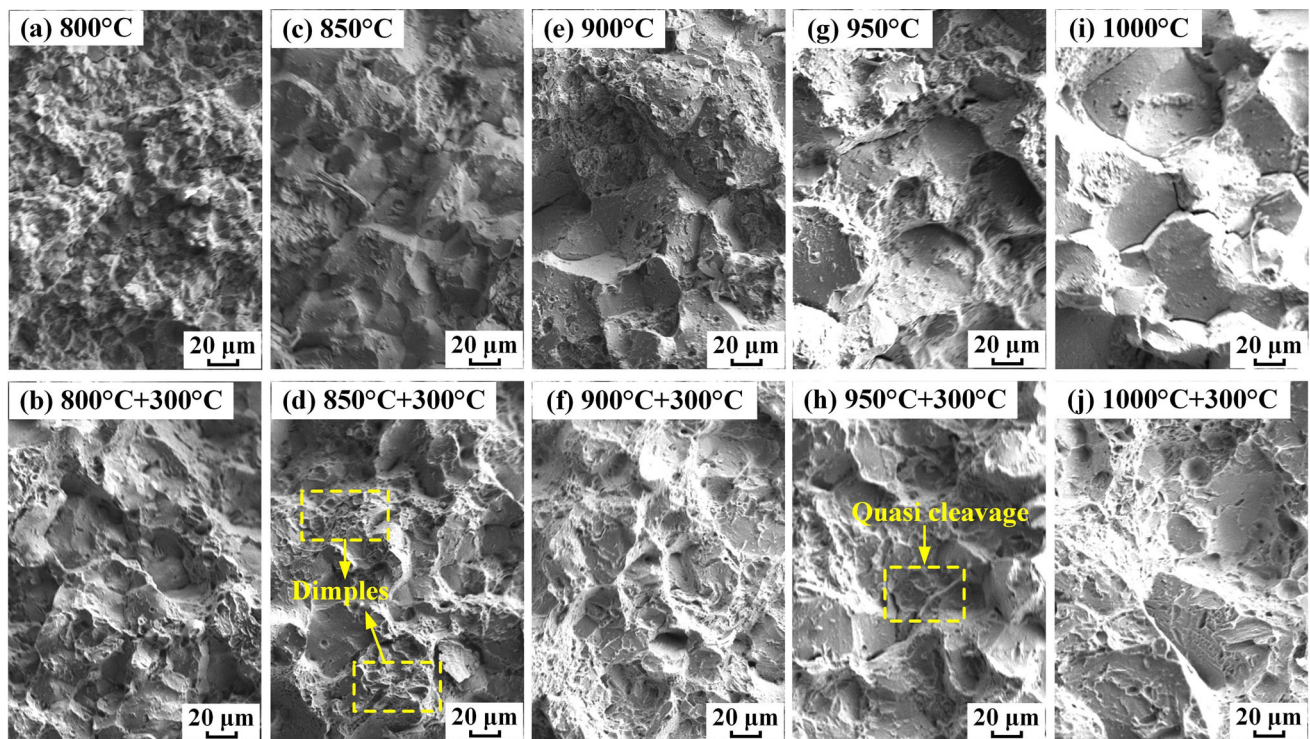


Fig. 9 Tensile fracture morphology under different heat treatment conditions: (a) 800 °C quenched and untempered, (b) 800 °C quenched and 300 °C tempered, (c) 850 °C quenched and untempered, (d) 850 °C quenched and 300 °C tempered, (e) 900 °C quenched and untempered, (f) 900 °C quenched and 300 °C tempered, (g) 950 °C quenched and untempered, (h) 950 °C quenched and 300 °C tempered, (i) 1000 °C quenched and untempered, and (j) 1000 °C quenched and 300 °C tempered

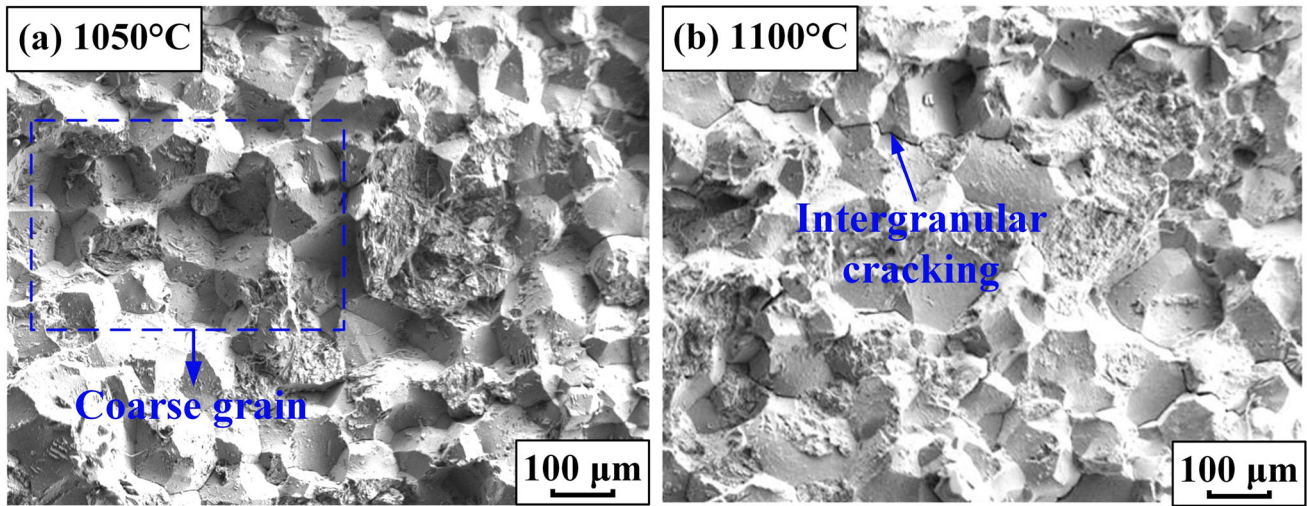


Fig. 10 Tensile fracture morphology of samples quenched at (a) 1050 °C and (b) 1100 °C

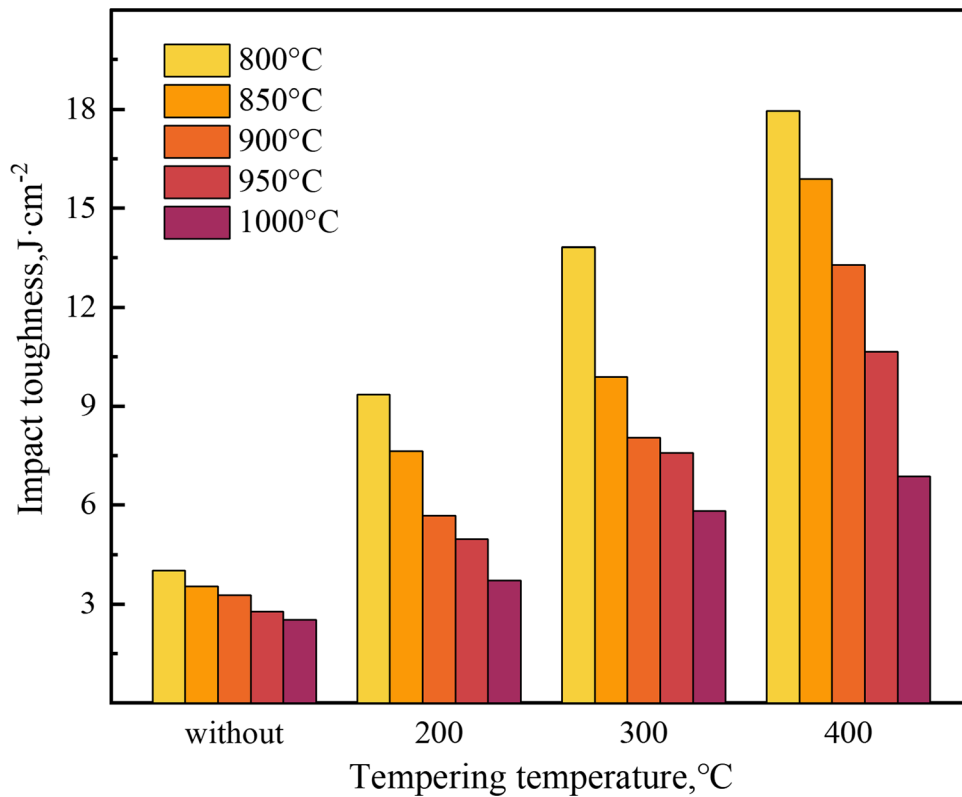


Fig. 11 Impact toughness under different heat treatment conditions

of the untempered samples is primarily brittle fracture, the impact fracture exhibits apparent intergranular fracture characteristics, the grain size increases with increasing quenching temperature, and the fracture presents varying degrees of grain polyhedron shape and rock-like pattern. When tempered at 300 °C, the sample exhibits a mixed tough-brittle fracture, and some ductile fracture characteristics were observed after tempering, with some small-sized dimples and tearing ridges.

According to Fig. 12(b), (d) and (f), when the quenching temperature does not exceed 900 °C, the toughness of the material can be improved by tempering, and the characteristics of intergranular fracture on the impact fracture are weakened. If the temperature for quenching reaches or exceeds 950 °C, the austenite grains become excessively coarse, rendering impact samples unable to improve in toughness by tempering. Obvious rock sugar-like grains can be observed in the impact fracture

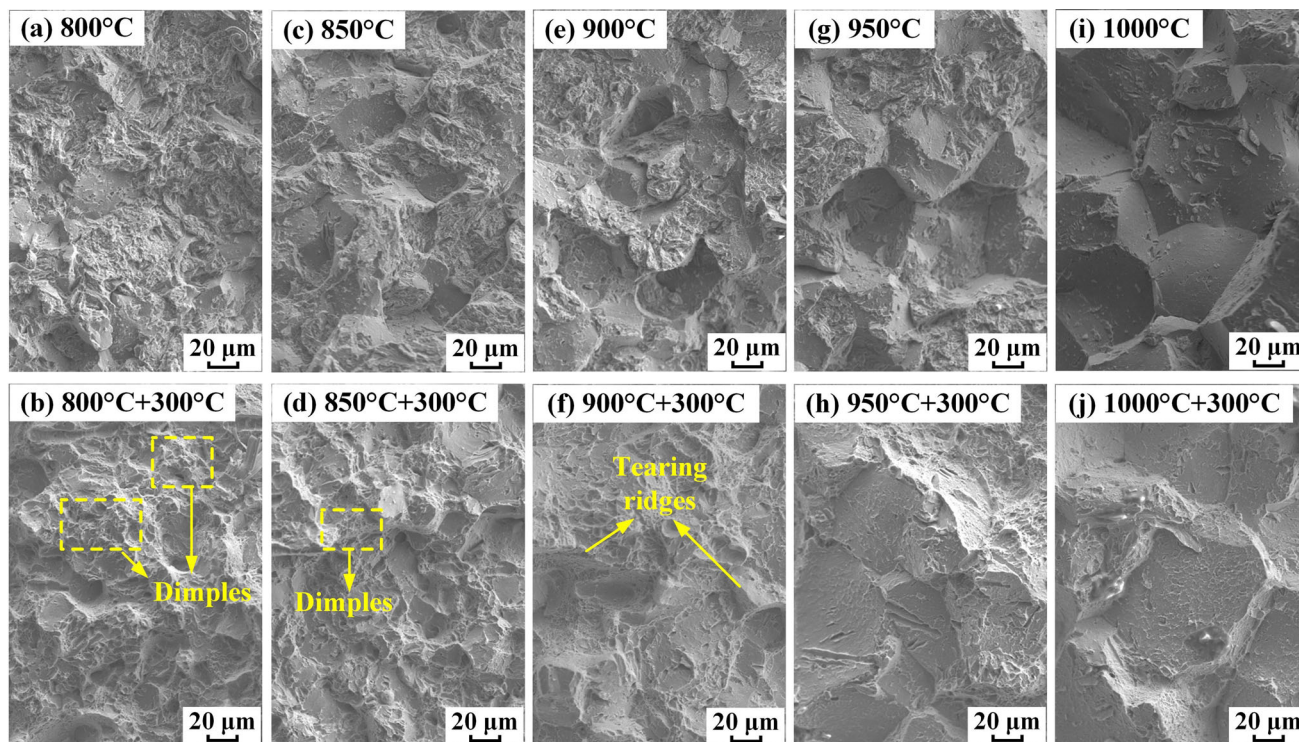


Fig. 12 Impact fracture morphology under different heat treatment conditions: (a) 800 °C quenched and untempered, (b) 800 °C quenched and 300 °C tempered, (c) 850 °C quenched and untempered, (d) 850 °C quenched and 300 °C tempered, (e) 900 °C quenched and untempered, (f) 900 °C quenched and 300 °C tempered, (g) 950 °C quenched and untempered, (h) 950 °C quenched and 300 °C tempered, (i) 1000 °C quenched and untempered, and (j) 1000 °C quenched and 300 °C tempered

before and after tempering, which can lead to the decline in comprehensive mechanical performance of the material, as well as a reduction in wear resistance, accuracy retention and service life.

Considering the hardness, tensile strength, impact toughness, and fracture morphology of tensile and impact samples, to ensure the high strength and toughness of the material, the optimal induction quenching temperature was finally determined to be 850-900 °C, in which the grain size is moderate, the hardness value is higher, and the comprehensive mechanical performance of the material is better. The optimal tempering temperature was determined to be 300 °C. The tensile strength of the 300 °C tempered sample is the highest, the toughness is relatively good, and the hardness value can meet the technical requirements of the actual production for linear guides.

4. Conclusions

- (1) As the quenching temperature remains constant, the hardness of untempered and 200 °C tempered samples are higher, while the hardness values of 300 and 400 °C tempered samples decrease with increasing tempering temperature.
- (2) Tensile strength values of untempered and 200 °C tempered samples are lower and the difference is not significant, increasing significantly after being tempered at 300 °C, which is approximately 2 to 3 times those of untempered samples, and then decreasing slightly after being tempered at 400 °C.

- (3) As the tempering temperature remains constant, the impact toughness values steadily decline as the quenching temperature rises, whereas when the quenching temperature remains constant, the impact toughness increases as the tempering temperature rises.
- (4) The optimum induction quenching temperature was finally determined to be 850-900 °C, and the optimum tempering temperature was 300 °C, in which the comprehensive mechanical performance of the material is excellent and can meet the technical requirements of the actual production for linear guides.

Acknowledgments

This research was funded by the National Natural Science Foundation of China (52175342), The Natural Science Foundation of Shandong (ZR2021ME129), the National Natural Science Foundation of China (52005304), Science and Technology Plan for Youth Innovation Team in Colleges and Universities of Shandong Province (2022KJ219).

Data Availability

The raw/processed data required to reproduce these findings cannot be shared at this time as the data also forms part of an ongoing study.

Conflict of interest

The authors declare no conflict of interest.

References

1. J. Li, Y. Ran, H.W. Wang, G.Q. Huang, Z.Y. Mu, and G.B. Zhang, Dynamic Performance Reliability Analysis of Rolling Linear Guide under Parameter Uncertainty, *J. Mech. Sci. Technol.*, 2020, **34**(11), p 4525–4536.
2. W. Sun, X.X. Kong, B. Wang, and X.Z. Li, Statics Modeling and Analysis of Linear Rolling Guideway Considering Rolling Balls Contact, *Proc. Inst. Mech. Eng. Part C-J. Eng. Mech. Eng. Sci.*, 2015, **229**(1), p 168–179.
3. X.Y. Wang, H.T. Feng, C.G. Zhou, and K.Q. Ye, A Thermal Model for Real-Time Temperature Forecast of Rolling Linear Guide considering Loading Working Conditions, *Int. J. Adv. Manuf. Technol.*, 2020, **109**, p 2249–2271.
4. X.Y. Wang, C.G. Zhou, and Y. Ou, Experimental Analysis of the Wear Coefficient for the Rolling Linear Guide, *Adv. Mech. Eng.*, 2019, **11**(1), p 1687814018821744.
5. C.Y. Li, M.T. Xu, G.K. He, H.Z. Zhang, Z.D. Liu, D. He, and Y.M. Zhang, Time-Dependent Nonlinear Dynamic Model for Linear Guideway with Crowning, *Tribol. Int.*, 2020, **151**, p 106413.
6. C.G. Zhou, S.H. Ren, H.T. Feng, J.W. Shen, Y.S. Zhang, and Z.T. Chen, A New Model for the Preload Degradation of Linear Rolling Guide, *Wear*, 2021, **482**, p 203963.
7. Y.Q. Wang, B.T. Liu, and Z.C. Guo, Wear Resistance of Machine Tools' Bionic Linear Rolling Guides by Laser Cladding, *Opt. Laser Technol.*, 2017, **91**, p 55–62.
8. C. Lorenzo-Martin and O.O. Ajayi, Rapid Surface Hardening and Enhanced Tribological Performance of 4140 Steel by Friction Stir Processing, *Wear*, 2015, **332**, p 962–970.
9. H. Purwanto, M. Dzulfikar, M. Tauviqirrahman, R. Ismail, and A. Jumain, The Effect of Austenitization Temperature in Surface Hardening Process on Steel Plate as Ballistic Plate, *J. Phys. Conf. Ser.*, 2021, **1908**(1), p 012030.
10. J.K. Choi, K.S. Park, and S.S. Lee, Prediction of High-Frequency Induction Hardening Depth of an AISI 1045 Specimen by Finite Element Analysis and Experiments, *Int. J. Precis. Eng. Manuf.*, 2018, **19**(12), p 1821–1827.
11. H. Li, H. Zhou, P. Zhang, T. Zhou, W. Su, S.Y. Wang, and H.F. Zhang, Influence of Laser Energy Density on Acquisition and Wear Resistance of Bionic Semisolid unit of 40Cr Steel, *J. Mater. Eng. Perform.*, 2020, **29**(4), p 2283–2295.
12. J. Liu, C. Wang, J. Zhong, Y. Wu, S.Y. Mo, and C.X. Gu, Microstructure and Properties of 45 Steel After Laser transformation Hardening and Induction Heating Surface Hardening, *Trans. Mater. Heat Treat.*, 2018, **39**(11), p 58–66.
13. D.C. Feng, J.X. Cui, X.X. Sun, and X.F. Wu, Effects of Induction and Traditional Tempering at Low Temperature on Microstructure and Properties of 45 Steel Tubes, *Hot Work. Technol.*, 2019, **48**(2), p 171–174.
14. J. Li, Z.X. Cao, L. Liu, X.D. Liu, and J. Peng, Effect of Microstructure on Hardness and Wear Properties of 45 Steel After Induction Hardening, *Steel Res. Int.*, 2021, **92**(4), p 2000540.
15. K. Kurek and D.M. Dolega, Numerical Simulation of Superficial Induction Hardening Process, *Int. J. Mater. Prod. Technol.*, 2007, **29**(1–4), p 84–102.
16. H.P. Li, L.F. He, K. Gai, R. Jiang, C.Z. Zhang, and M.S. Li, Numerical Simulation and Experimental Investigation on the Induction Hardening of a Ball Screw, *Mater. Des.*, 2015, **87**, p 863–876.
17. J. Grum, A Review of the Influence of Grinding Conditions on Resulting Residual Stresses After Induction Surface Hardening and Grinding, *J. Mater. Process. Technol.*, 2001, **114**(3), p 212–226.
18. V. Rudnev, Induction Hardening of Gears and Critical Components, *Gear. Technol.*, 2008, p 58–63.
19. R.M. Horn and R.O. Ritchie, Mechanisms of Tempered Martensite Embrittlement in Low Alloy Steels, *Metall. Trans. A*, 1978, **9**, p 1039–1053.
20. A. Salemi and A. Abdollah-zadeh, The Effect of Tempering Temperature on the Mechanical Properties and Fracture Morphology of a NiCrMoV Steel, *Mater. Charact.*, 2008, **59**(4), p 484–487.
21. F.G. Liu, X. Lin, M.H. Song, H.O. Yang, K. Song, P.F. Guo, and W.D. Huang, Effect of Tempering Temperature on Microstructure and Mechanical Properties of Laser Solid Formed 300M Steel, *J. Alloys Compd.*, 2016, **689**, p 225–232.
22. S. Maropoulos, S. Karagiannis, and N. Ridley, The Effect of Austenitising Temperature on Prior Austenite Grain Size in a Low-Alloy Steel, *Mater. Sci. Eng. A*, 2008, **483**, p 735–739.
23. J.M. Han, S.H. Cui, W.J. Li, and X.Y. Ma, Dual Phase Heat Treatment of Low-Alloy Steel, *J. Iron. Steel Res. Int.*, 2005, **12**(5), p 47–51.
24. J. Wang, Z.N. Xu, and X.F. Lu, Effect of the Quenching and Tempering Temperatures on the Microstructure and Mechanical Properties of H13 Steel, *J. Mater. Eng. Perform.*, 2020, **29**(3), p 1849–1859.
25. W. Cheng, X.L. Zhang, J.Z. Lu, F.Z. Dai, and K.Y. Luo, Effect of Laser Oscillating Welding on Microstructure and Mechanical Properties of 40Cr steel/45 Steel Fillet Welded Joints, *Optik*, 2021, **231**, p 166458.
26. G. Krauss, Deformation and Fracture in Martensitic Carbon Steels Tempered at Low Temperatures, *Metall. Mater. Trans. B*, 2001, **32**, p 205–221.
27. X.D. Liang, J.W. Lü, H. Yan, Z.J. Zhao, X.Y. Wang, J.M. Meng, and X. Wang, Effect of Tempering Temperature on Microstructure and Mechanical Properties of C61 Gear Steel, *Trans. Mater. Heat Treat.*, 2022, **43**(1), p 84–91.
28. C. Sun, P.X. Fu, H.W. Liu, H.H. Liu, and N.Y. Du, Effect of Tempering Temperature on the Low Temperature Impact Toughness of 42CrMo4-V Steel, *Metals*, 2018, **8**(4), p 232.
29. P. Yan, Z.D. Liu, H.S. Bao, Y.Q. Weng, and W. Liu, Effect of Tempering Temperature on the Toughness of 9Cr-3W-3Co Martensitic Heat Resistant Steel, *Mater. Des.*, 2014, **54**, p 874–879.

Publisher's Note Springer Nature remains neutral with regard to jurisdictional claims in published maps and institutional affiliations.

Springer Nature or its licensor (e.g. a society or other partner) holds exclusive rights to this article under a publishing agreement with the author(s) or other rightsholder(s); author self-archiving of the accepted manuscript version of this article is solely governed by the terms of such publishing agreement and applicable law.